

# Dynamical coupled-channels study of meson production reactions from EBAC@JLab

Hiroyuki Kamano

*Excited Baryon Analysis Center (EBAC), Thomas Jefferson National Accelerator Facility, Newport News, VA 23606, USA*

**Abstract.** We present the current status of a combined and simultaneous analysis of meson production reactions based on a dynamical coupled-channels (DCC) model, which is conducted at Excited Baryon Analysis Center (EBAC) of Jefferson Lab.

**Keywords:** Dynamical coupled-channels analysis, meson production reactions

**PACS:** 14.20.Gk, 13.75.Gx, 13.60.Le

## INTRODUCTION

An understanding of the spectrum and structure of the excited nucleon ( $N^*$ ) states is a fundamental challenge in the hadron physics. The  $N^*$  states, however, couple strongly to the meson-baryon continuum states and appear only as resonance states in  $\pi N$  and  $\gamma N$  reactions. Such strong couplings to the meson-baryon continuum states influence significantly the  $N^*$  properties and cannot be neglected in extracting the  $N^*$  parameters from the data and giving physical interpretations. It should also be emphasized that at present even the existence is still uncertain for most of the  $N^*$  states higher than 1.6 GeV [1]. This will be because most of the  $N^*$  information were extracted only from the  $\pi N \rightarrow \pi N$  and  $\gamma N \rightarrow \pi N$  analysis. It is thus well recognized nowadays that the comprehensive study of *all* relevant meson production reactions with  $\pi N$ ,  $\eta N$ ,  $\pi\pi N$ ,  $KY$ ,  $\omega N$ ,  $\dots$  final states based on a coupled-channels framework is inevitable for reliable extraction of such higher  $N^*$  states.

To make a progress to this direction, the Excited Baryon Analysis Center (EBAC) of Jefferson Lab is conducting a dynamical coupled-channels (DCC) analysis of  $\pi N$ ,  $\gamma N$ , and  $N(e, e')$  reactions in the resonance region. The analysis is based on an unitarized coupled-channels model, the EBAC-DCC model (see Ref. [2] for the details), within which the couplings among relevant meson-baryon reaction channels are fully taken into account.

In this model, the reaction amplitudes  $T_{\alpha,\beta}(p, p'; E)$  are calculated from the following coupled-channels integral equations,

$$T_{\alpha,\beta}(p, p'; E) = V_{\alpha,\beta}(p, p') + \sum_{\gamma} \int_0^{\infty} q^2 dq V_{\alpha,\gamma}(p, q) G_{\gamma}(q, E) T_{\gamma,\beta}(q, p', E), \quad (1)$$

$$V_{\alpha,\beta} = v_{\alpha,\beta} + \sum_{N^*} \frac{\Gamma_{N^*,\alpha}^{\dagger} \Gamma_{N^*,\beta}}{E - M^*}, \quad (2)$$

where  $\alpha, \beta, \gamma = \gamma N, \pi N, \eta N, \pi\pi N, K\Lambda, K\Sigma, \omega N$  (the  $\pi\pi N$  channel contains the quasi two-body  $\pi\Delta, \rho N, \sigma N$  channels);  $v_{\alpha,\beta}$  is a meson-exchange interaction including only ground state mesons and baryons, which is derived from phenomenological Lagrangians;  $\Gamma_{N^*,\beta}$  describes the excitation of the nucleon to a bare  $N^*$  state with a mass  $M^*$ ;  $G_{\gamma}(q, E)$  is the meson-baryon Green function for the channel  $\gamma$ . The second term of Eq. (2) thus describes the  $s$ -channel exchange of bare  $N^*$  states. Through the reaction processes, the bare  $N^*$  states couple to the meson-baryon continuum states (reactions channels) and become resonance states. On the other hand, the meson-exchange potential  $v_{\alpha,\beta}$  can also generate molecule-like resonances dynamically. The physical nucleon resonances will be a ‘‘superposition’’ of these two pictures in general.

During the developing stage of EBAC in 2006-2009, hadronic and electromagnetic parameters of the EBAC-DCC model were determined by analyzing  $\pi N \rightarrow \pi N$  [3] and  $\pi N \rightarrow \eta N$  [4] up to  $W = 2$  GeV, and  $\gamma N \rightarrow \pi N$  [5] and  $N(e, e'\pi)N$  [6] up to  $W = 1.6$  GeV. Then, the model was applied to  $\pi N \rightarrow \pi\pi N$  [7] and  $\gamma N \rightarrow \pi\pi N$  [8] to predict cross sections and examine consistency of the coupled-channels framework. Also, nucleon resonance poles were extracted from the model and a new interpretation for the dynamical origin of  $P_{11}$  nucleon resonances was proposed [9].

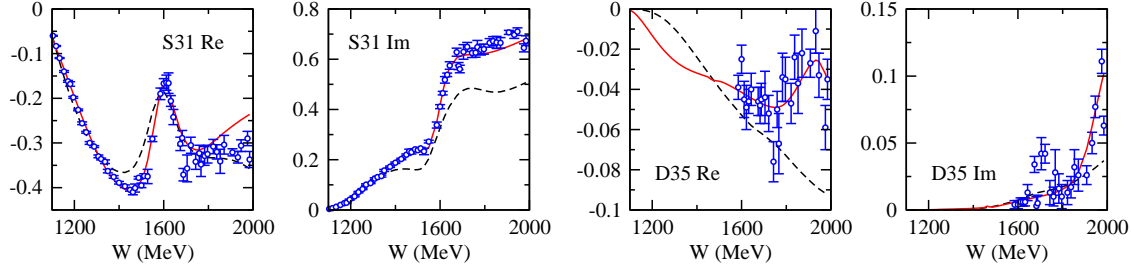


**FIGURE 1.** The partial wave amplitudes of the  $\pi N$  scattering. (Red solid curves) The current result (*preliminary*). (Black dashed curves) Our previous model [3]. The data points are the energy-independent solution of SAID, which are taken from Ref. [10].

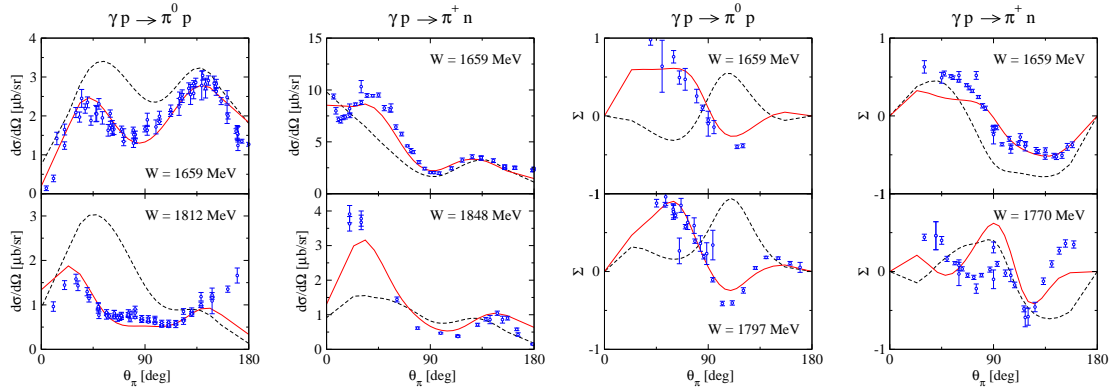


**FIGURE 2.** The differential cross sections (left two columns) and the photon asymmetry (right two columns) of the  $\gamma p \rightarrow \pi^0 p, \pi^+ n$  reactions at high energies  $W > 1.6$  GeV. (Red solid curves) The current result (*preliminary*). (Black dashed curves) Our previous model [5]. The data are taken from the database of Ref. [10].

Although the model constructed in the early analysis successfully describes the data in the wide energy region, it is still far from our goal because only  $\pi N$  and  $\eta N$  channels are taken into account in the fit and each reaction is analyzed rather separately (e.g., in the analysis of  $\gamma N \rightarrow \pi N$ , the hadronic parameters fitted to the  $\pi N$  scattering data are used and, only the electromagnetic parameters are varied). To proceed further, we have started a full combined analysis of  $\pi N$ ,  $\eta N$ ,  $\pi\pi N$ ,  $KY$ ,  $\omega N$  channels recently, in which all parameters are varied simultaneously. We are currently performing a combined analysis of  $\pi N$ ,  $\gamma N \rightarrow \pi N$ ,  $\eta N$ ,  $K\Lambda$ ,  $K\Sigma$  reactions as a first step. In this contribution, we present the status of our current effort for the analysis.

## CURRENT STATUS OF THE EBAC-DCC ANALYSIS

The  $\pi N \rightarrow \pi N$  and  $\gamma N \rightarrow \pi N$  reactions: The partial wave amplitudes of the  $\pi N$  scattering are shown in Fig. 1. Here we present only the result of two partial waves,  $S_{31}$  and  $D_{35}$ , where a significant improvement has been achieved from our early model [3]. Other partial waves are the same quality as the early model. The improvement in the  $D_{35}$  partial wave is mainly due to an inclusion of one bare  $N^*$  state.

The current  $\gamma N \rightarrow \pi N$  analysis has two major progresses over our previous analysis constructed in Ref. [5]: (a) the energy region for the analysis is extended from  $W \leq 1.6$  GeV to  $W \leq 2$  GeV, and (b) data of the unpolarized differential cross section and all measured polarization observables are taken into account in the fit, while only differential cross sections and photon asymmetry  $\Sigma$  are used in our previous analysis. In Fig. 2, our preliminary result (red solid curves) of  $\gamma N \rightarrow \pi N$  at the energies  $W > 1.6$  GeV is compared to our previous model (black dashed curves) as well as the experimental data. We can actually observe a visible improvement of the model in  $W > 1.6$  GeV.

The  $\pi N \rightarrow \eta N$  reaction: It is known that for the  $\pi^- p \rightarrow \eta n$  reaction underlying inconsistencies exist among data sets from different experimental groups [4]. In our analysis, we follow the strategy described in Ref. [4] for how to

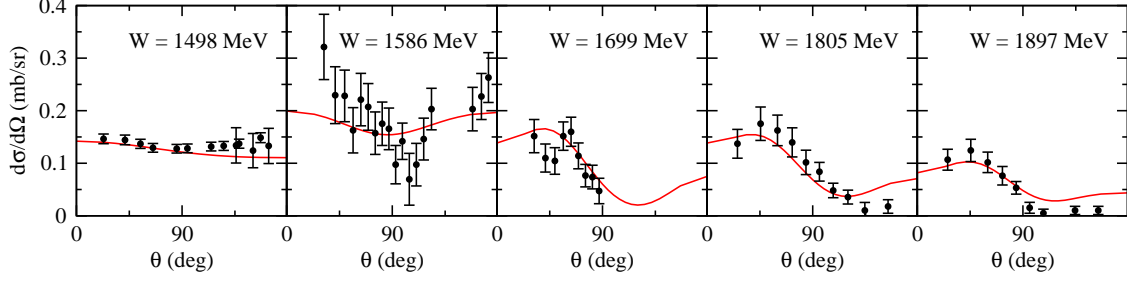


**FIGURE 3.** The differential cross sections of the  $\pi^- p \rightarrow \eta n$  reactions. Red solid curves are the current result (*preliminary*). See Ref. [4] for the details of the data used.

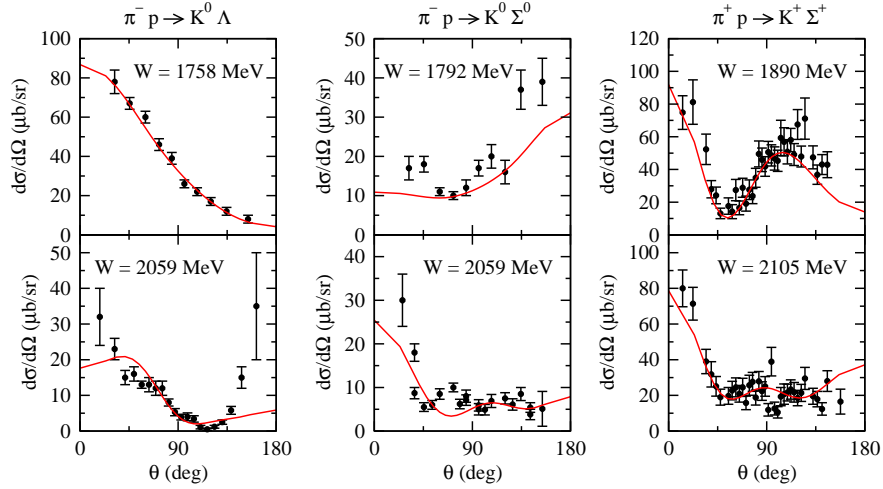


**FIGURE 4.** The preliminary result for the differential cross sections of  $\pi^+ p \rightarrow K^+ \Sigma^+$  (left panels),  $\pi^- p \rightarrow K^0 \Sigma^0$  (middle panels), and  $\pi^- p \rightarrow K^0 \Lambda^0$  (right panels). The data are from Refs. [11, 12].

select the data to be used for our analysis. In Fig. 3, we present the current status of the  $\pi^- p \rightarrow \eta n$  reactions. We find that at present our result describes reasonably well the differential cross section data up to  $W = 1.9$  GeV. The analysis of  $\gamma p \rightarrow \eta p$  is also underway.

The  $\pi N \rightarrow KY$  and  $\gamma N \rightarrow KY$  reactions: Now we move to showing the current status of the analysis for the  $KY$  reactions. In Fig. 4, we present the differential cross sections of the  $\pi N \rightarrow KY$  reactions for three different charge states. At present we have included the data up to  $W = 2.1$  GeV for the analysis. The current result describes the data of the considered energy region reasonably well.

Finally, we present the current status of the  $\gamma p \rightarrow K^+ \Lambda$  analysis. This strangeness-production reaction is expected to be one of the most promising reactions to provide critical information for confirming/rejecting not well-established  $N^*$ s and/or discovering new  $N^*$ s. Because of this, measurement of the polarization observables, which are more exclusive than unpolarized cross section, for  $\gamma p \rightarrow K^+ \Lambda$  becomes very active at electron beam facilities. For example, first measurement of the  $O_x$ ,  $O_z$ , and  $T$  asymmetries has been reported recently by GRAAL [16]. Furthermore, the so-called “(over-) complete experiments” is planned at CLAS, in which *all* 15 polarization observables are measured, and so extensive data will be available in near future.

In Fig. 5, the differential cross sections and the polarization observables  $P, C_x, C_z$  are compared with those measured in the CLAS-g11a [14] and CLAS-g1c [15] experiments. Here we note that care must be taken in calculating the polarization observables because incompatibility exist in the expressions of the observables in the literature (see Ref. [13] for the detail). In our analysis, we follow the definitions explicitly described in Ref. [13]. Although it must be further improved, our model describes qualitatively the available differential cross sections and polarization

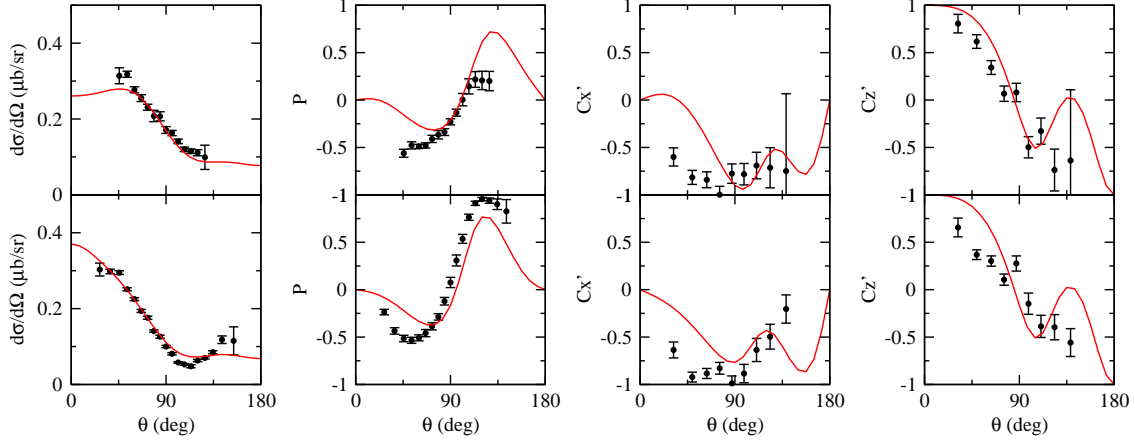


**FIGURE 5.** The preliminary result for the differential cross sections and  $P$ ,  $C_{x'}$ , and  $C_{z'}$  asymmetries of  $\gamma p \rightarrow K^+ \Lambda$ . The upper (lower) panels are the result at  $E_\gamma = 1250$  MeV ( $E_\gamma = 1650$  MeV). The data are from Refs. [14, 15].

observables. In order to describe the data of all polarization observables measured in upcoming experiments at CLAS, however, we may need to introduce additional bare  $N^*$  states to reproduce such extensive data. Then the introduced bare  $N^*$  states may generate new resonance states.

In summary, the Excited Baryon Analysis Center of Jefferson Lab makes a continuous effort for a combined and simultaneous coupled-channels analysis of all relevant meson-production reactions toward the ultimate goal of establishing the  $N^*$  spectrum and extracting  $N^*$  parameters. We are currently performing a combined analysis of the  $\pi N$ ,  $\gamma N \rightarrow \pi N, \eta N, K\Lambda, K\Sigma$  reactions. Although further improvements are necessary, our current model describes the reactions reasonably well from threshold up to  $W \sim 2$  GeV. Once this analysis is completed, we will gradually extend our analysis by including other reactions with final states such as  $\pi\pi N$  and  $\omega N$ .

## ACKNOWLEDGMENTS

The author would like to thank B. Juliá-Díaz, T.-S. H. Lee, A. Matsuyama, S. X. Nakamura, T. Sato, and N. Suzuki for their collaborations at EBAC. This work was supported by the U.S. Department of Energy, Office of Nuclear Physics Division, under Contract No. DE-AC05-06OR23177 under which Jefferson Science Associates operates the Jefferson Lab.

## REFERENCES

1. R. A. Arndt, W. J. Briscoe, I. I. Strakovsky, and R. L. Workman, *Phys. Rev. C* **74**, 045205 (2006).
2. A. Matsuyama, T. Sato, and T.-S. H. Lee, *Phys. Rep.* **439**, 193 (2007).
3. B. Juliá-Díaz, T.-S. H. Lee, A. Matsuyama, and T. Sato, *Phys. Rev. C* **76**, 065201 (2007).
4. J. Durand, B. Juliá-Díaz, T.-S. H. Lee, B. Saghai, and T. Sato, *Phys. Rev. C* **78**, 025204 (2008).
5. B. Juliá-Díaz, T.-S. H. Lee, A. Matsuyama, and T. Sato, and L. C. Smith, *Phys. Rev. C* **77**, 045205 (2008).
6. B. Juliá-Díaz, H. Kamano, T.-S. H. Lee, A. Matsuyama, T. Sato, N. Suzuki, *Phys. Rev. C* **80**, 025207 (2009).
7. H. Kamano, B. Juliá-Díaz, T.-S. H. Lee, A. Matsuyama, and T. Sato, *Phys. Rev. C* **79**, 025206 (2009).
8. H. Kamano, B. Juliá-Díaz, T.-S. H. Lee, A. Matsuyama, and T. Sato, *Phys. Rev. C* **80**, 065203 (2009).
9. N. Suzuki, B. Julia-Díaz, H. Kamano, T.-S. H. Lee, A. Matsuyama, T. Sato, *Phys. Rev. Lett.* **104**, 042302 (2010).
10. CNS Data Analysis Center, GWU, <http://gwdac.phys.gwu.edu>.
11. B. Juliá-Díaz, B. Saghai, T.-S. H. Lee, F. Tabakin, *Phys. Rev. C* **73**, 055204 (2006), references therein.
12. D. J. Candlin *et al.*, *Nucl. Phys.* **B226**, 1 (1983).
13. A. Sandorfi, S. Hoblit, H. Kamano, T.-S. H. Lee, arXiv:0912.3505 [nucl-th]; in preparation.
14. M. E. McCracken *et al.* (CLAS collaboration), *Phys. Rev. C* **81**, 025201 (2010).
15. R. K. Bradford *et al.* (CLAS collaboration), *Phys. Rev. C* **75**, 035205 (2007).
16. A. Lleres *et al.* (GRAAL collaboration), *Eur. Phys. J. A* **39**, 149 (2009).